

## Fracture Analyses of the Early Cambrian Ambar Formation, at Ambar village, district Swabi Pakistan: in regional tectonic perspective.

Asghar Ali<sup>1</sup>, Mohammad Noor Taj Khan<sup>1</sup>, Taj Mohammad Wazir<sup>1</sup> and Sajjad Ahmad<sup>1</sup>

### ABSTRACT

An evaluation of fractures in the Early Cambrian Ambar Formation was conducted to ascertain the tectonic setup of the study area in regional tectonic context. It enables to understand large-scale tectonic dynamic processes that developed at the northwest Indo-Pakistan tectonic plate through time. Fracture analyses reveal that these rocks have been affected by at least two regional scale deformation events. Extension fractures of the Ambar Formation indicate the early history of tectonism, which pre-dates the Cenozoic Himalayan Orogeny. Microscopic study of the infilling secondary minerals and their internal structures in relation to fracture walls indicate that these fractures belong to Mode I extension fractures. Similarly the mechanism of crystal growth in en-echelon veins and the geometry of their arrays further support the extensional nature of these fractures. The remarkable resemblance among the trends of these extension fractures, normal faults in the south central Swat, Peshawar Basin and rift related intrusive bodies suggest that these fractures developed during the Late Paleozoic intra-continental rifting. Later deformation of these fractures and overall increase in fracture density in the rocks occurred during the Himalayan Orogeny.

### INTRODUCTION

Fracturing of rocks at the upper crust is a fundamental mechanism of brittle failure (Paterson, 1978; Hancock, 1985; Ramsay and Huber, 1987; Ranalli, 1995; Ramsey and Chester, 2004). Fractures and veins with characteristic patterns contain enormous information on the existing stress and strain fields during their formation (Ramsay and Huber, 1987; Price and Cosgrove, 1990; Oliver and Bons, 2001). Such structures can help in measuring the stress orientations existing at the time of their formation (Ramsay and Huber, 1987; Price and Cosgrove, 1990; Oliver and Bons, 2001; Koehn et al., 2005).

Fractures are of the three types on the basis of their mode of opening. Mode I fractures are extensional in nature (Paterson, 1978; Jaeger and Cook, 1979; Ramsay, 1980; Ramsay and Huber, 1987; Pollard and Aydin, 1988; Ranalli, 1995; Ramsey and Chester, 2004). Mode II are sheared fractures with shearing parallel to the fractured walls and Mode III fractures are hybrid with both extension perpendicular and shearing parallel to the fracture boundaries (Paterson, 1978; Ramsay and Huber, 1987; Ranalli, 1995; Ramsey and Chester, 2004; Figure 1). Mode I extension fractures are called joints without visible differential displacement (Davis, 1984; Ramsay and Huber, 1987; Pollard and Aydin, 1988). Systematic fractures are useful in interpreting the regional stress directions (Parker, 1942; Anderson, 1951; Engelder, 1982). These might be planar,

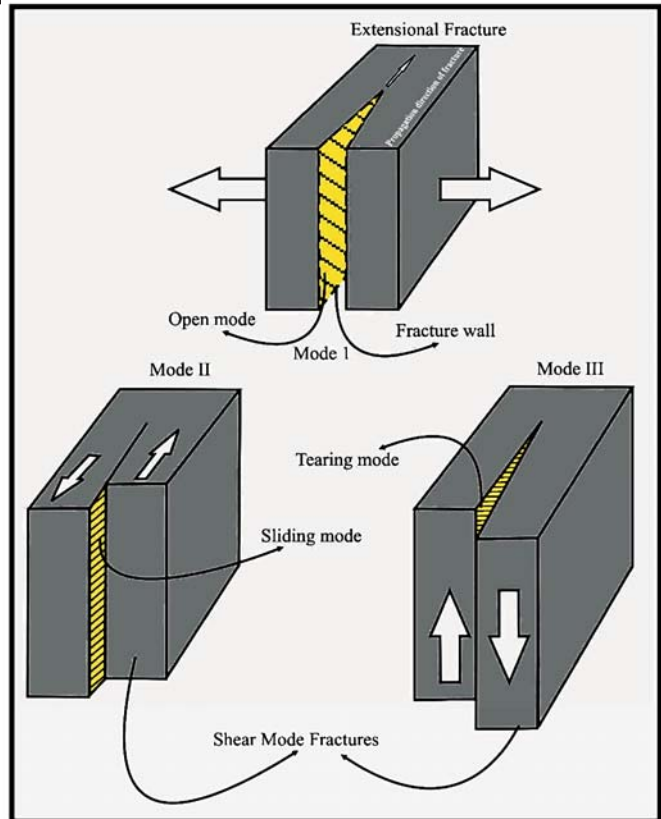


Figure 1- Schematic representation of the 3-D geometry of open and shear mode fractures during brittle deformation in a rock (modified after Twiss & Moores, 1992).

sub-parallel and evenly spaced, occurring in sets. In this paper we use fracture patterns of the Early Cambrian Ambar Formation at Ambar village to understand their tectonic evolution with time and to advance our understanding of rock deformation at all scales.

### GEOLOGICAL SETTING

The hinterland zone of the Northwest Himalayan fold-and-thrust belt (Figure 2) records two regional tectonic events. The extensional tectonic event during the Late Paleozoic time (Pogue et al., 1992a) and the compressional tectonic event in the Cenozoic time (Treloar et al., 1989). The pre and syn-rift metasedimentary rocks of the eastern Peshawar Basin and Swat (Figure 3) provide evidence for the Late Paleozoic rifting that occurred at the northern margin of the Indo-Pakistan tectonic plate. The pre-Himalayan clastic sedimentation of the Late Paleozoic-Triassic Jafar Kandao Formation specifies the beginning of extensional tectonics. The clastic input was derived from the formerly passive northern margin of the Gondwana Land (Pogue et al., 1992a). The Permian rift is accompanied by eruption of basaltic lava and alkaline

<sup>1</sup> Department of Geology, University of Peshawar, Pakistan.

Fracture Analyses of the Early Cambrian Ambar Formation

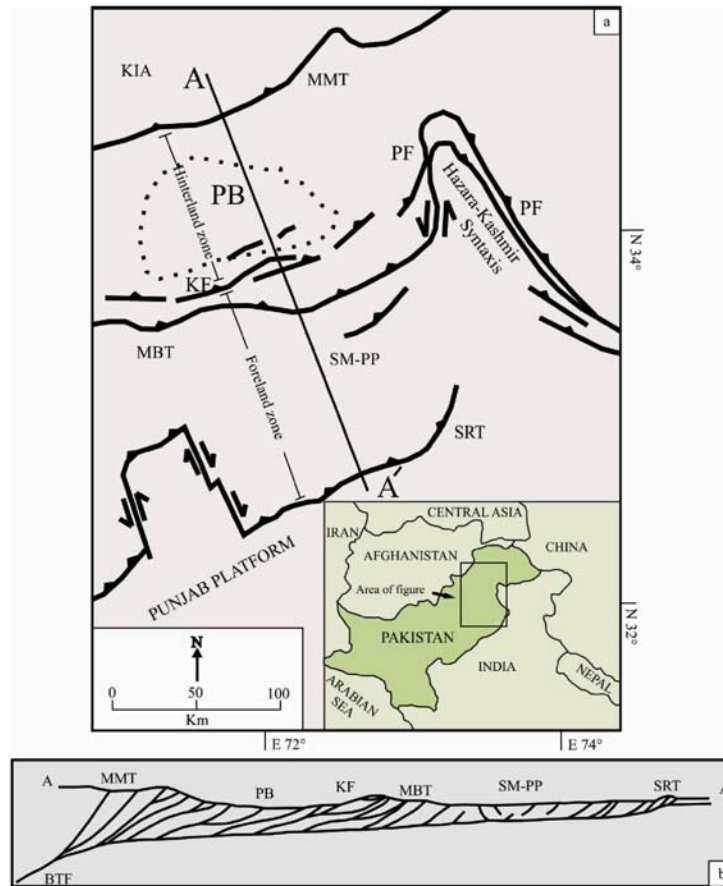


Figure 2- (a)Tectonic map of the northwest Himalayan fold-and-thrust belt. Thick lines represent regional faults. Dotted line encircles the Peshawar Basin; (b) Schematic cross section along the line A-A/ in (a), illustrating the style of deformation within this belt(after Burbank, 1983). KIA= Kohistan Island Arc; MMT= Main Mantle Thrust; PB= Peshawar basin; KF= Khairabad Fault; PF= Panjal Fault; MBT= Main Boundary Thrust; SM-PP= Siwalik Molasse-Potwar Plateau; SRT= Salt Range Thrust; BTF= Basement Thrust Front.

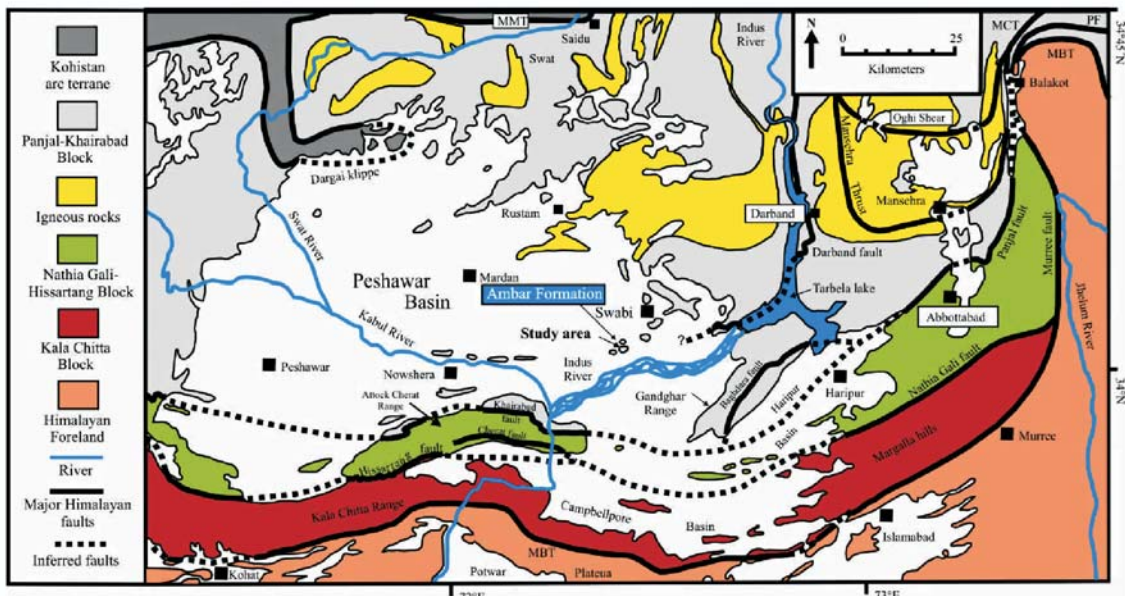


Figure 3 - Tectonic map of the Peshawar Basin and surroundings showing major Himalayan faults (after Hussain et al., 1991 and Pogue et al., 1999).

magmatism characterized by the Shewa-Shahbazgarhi, Warsak porphyries and Koga syenite (Pogue et al., 1992a).

The collision of Indian and Eurasian plates in the Cenozoic time has resulted in one of the most distinct global feature, the Himalayan Mountains. The Himalayan Orogeny is related with volcanism, magmatism, metamorphism and the formation of regional scale fold-and-thrust belts (Treloar et al., 1989). The north-south oriented stresses have resulted in extensive deformation along the northern margin of the Indo-Pakistan tectonic plate. The stresses developed in the course of collision are gradually released by the development of south-verging folds and thrust belts (Northwest Himalayan fold-and-thrust belt) at the northern margin of the Indian Plate (Yeats and Lawrence, 1984).

The Ambar Formation, which is the focus of the present study, crops out in the south-eastern part of the Peshawar Basin (Figure 3). The Peshawar Basin lies in the southwestern part of the hinterland zone. It has been classified as a piggyback-type basin because it has been carried passively on the back of low-angle detachment faults and thrust sheets, some of which find surface exposure in the hill ranges to the south of the Basin (Figure 3; Ori and Friend, 1984). The Basin is surrounded by the Precambrian metasediments and an almost complete fossiliferous Paleozoic sequence (DiPietro et al., 1999; Pogue et al., 1999). The basal Proterozoic sedimentary sequence (Table 1) of the Peshawar Basin consists of the Hazara (Dakhner), Gandaf, Manki and Tanawal Formations (DiPietro et al., 1999; Pogue et al., 1999). The Proterozoic basal sequence is overlain by the Paleozoic sequence, which consists of the Ambar, Misri Banda Quartzite, Panjpir, Nowshera, Jafar Kandao and Duma Formations (Pogue et al., 1992b; DiPietro et al., 1999; Pogue et al., 1999). The complete Paleozoic sequence is exposed in the ranges that are fringing the Peshawar Basin (Hussain et al., 1991; Pogue et al., 1992b).

The Ambar Formation consists of dolomite, dolomitic limestone, calcareous quartzite and subordinate argillite exposed in the isolated hills between Nowshera and Swabi regions (Figure 3). The Ambar Formation unconformably overlies the Late Proterozoic Tanawal Formation in the north and east of Swabi (Hussain et al., 1991; Pogue et al., 1992b). The contact between the Tanawal Formation and Ambar Formation is locally marked by a cobble or pebble conglomerate consisting of well-rounded quartzite clasts in the matrix that grades upward from quartzite or argillite to sandy dolomite (Pogue et al., 1992b). In the Peshawar Basin south of Swabi, the lower contact of the Ambar Formation is concealed beneath the alluvium of the Peshawar Basin. The unconformable contact with the overlying Misri Banda Quartzite is underlain by 5-10 m of argillite. It becomes thin in the northern suburbs of Swabi and is absent from the northern half of the Chingalai Synclinorium (Hussain et al., 1991). The Ambar Formation which is unfossiliferous, has been correlated with the Sirban Formation of the Lower Cambrian Abbottabad Group on the basis of stratigraphy and lithology (Pogue et al., 1999).

#### OUTCROP DESCRIPTION

Field observations and data were systematically collected across the Ambar Formation. The outcrop at Ambar village exposes the Paleozoic metasedimentary sequence of the hinterland zone (DiPietro et al., 1999; Pivnik and Wells, 1996), consisting of the Ambar, Misri Banda Quartzite, Panjpir and Nowshera Formations (Hussain et al., 1991).

The outcrop contains gently dipping beds with average dip values of 30° (Figure 4a). Mesoscopic folds in the study area deformed the tectonic veins of the Ambar Formation (Figures 4b and 5a, 5b). The competent dolomite beds of the Ambar Formation have undergone flexural slip folding, where the

Table 1- The generalized Early Proterozoic to Mesozoic stratigraphy of the Peshawar Basin (after DiPietro et al., 1999).

Age	Formation
Mesozoic	Nikanai Ghar
	Kashala
Late Paleozoic-Triassic	Duma
	Jafar Kandao
Early-Middle Paleozoic	Nowshera
	Panjpir
	Misri Banda
	Ambar
Late Proterozoic	Tanawal
Early Proterozoic	Gandaf, Manki and Hazara

inner arcs of the folds are deformed by minor thrust slip faults to accommodate the layer parallel shortening (cf. Davis and Reynolds, 1996; Ramsay, 1967). The whole region is lying in the low grade metamorphosed fold-and-thrust belt that formed during the Himalayan Orogeny (Kazmi and Jan, 1997).

The Ambar Formation is highly fractured with some fractures having systematic fracture pattern (Figure 6). The Ambar Formation was selected for data collection due to ease in accessibility, greater exposure and nature of the study.

## METHODOLOGY

Attitudes of one hundred and eighty-four fractures were recorded at eighteen stations where fractures were well exposed (Table 2; Figure 7). We recorded the data from every fracture at the outcrop, which were through going, clearly opened and planar. The general fracturing aspect, persistency, nature of mineral fillings and nature of fracture surfaces were recorded for each fracture. Attitudes of bedding at each station, bed thicknesses, lithology and other structures were also recorded.

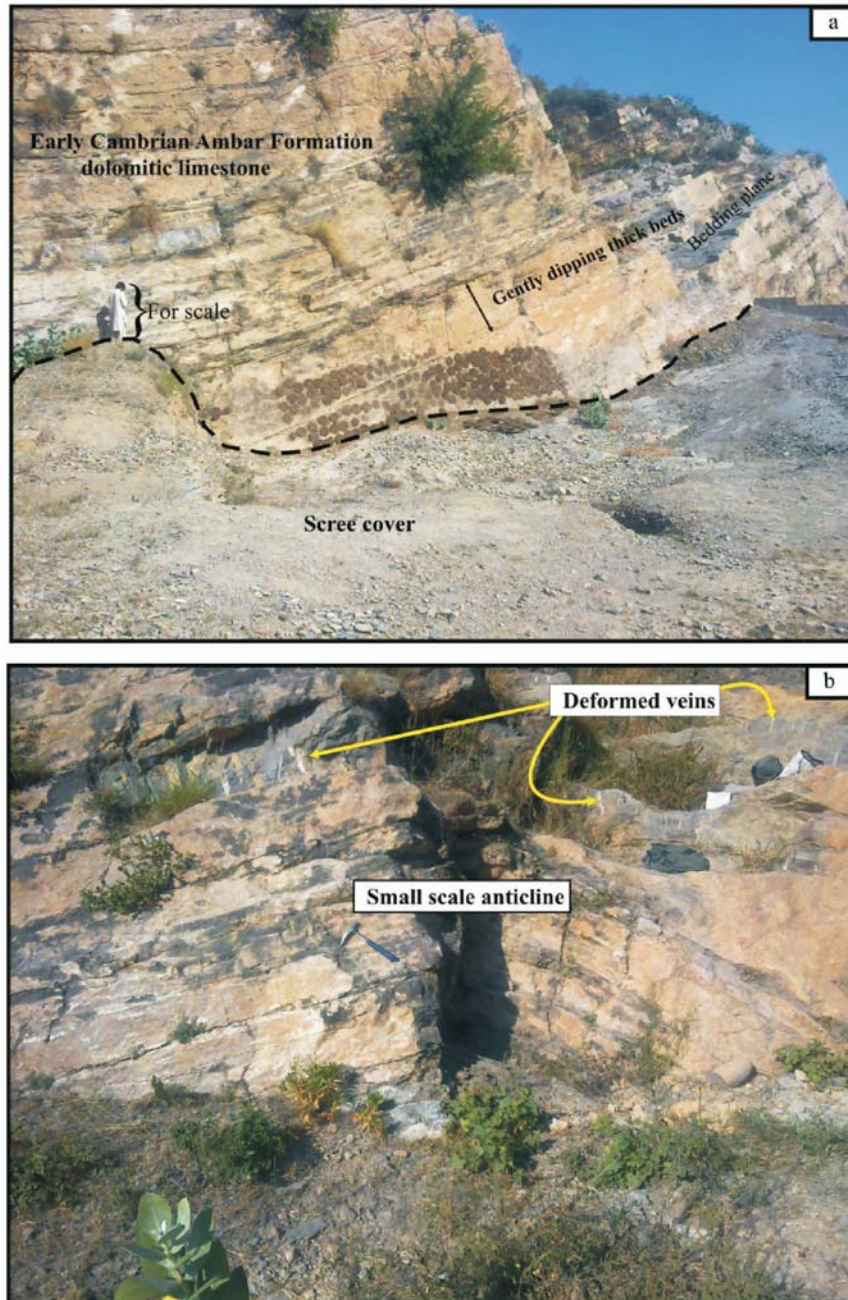


Figure 4 - (a) Photograph taken towards  $100^\circ$  showing beds of the Ambar Formation, which are dipping towards  $315^\circ$ . Below the dotted line, beds are scree covered. (b) Photograph taken towards  $50^\circ$  showing small scale intra formation anticline fold.

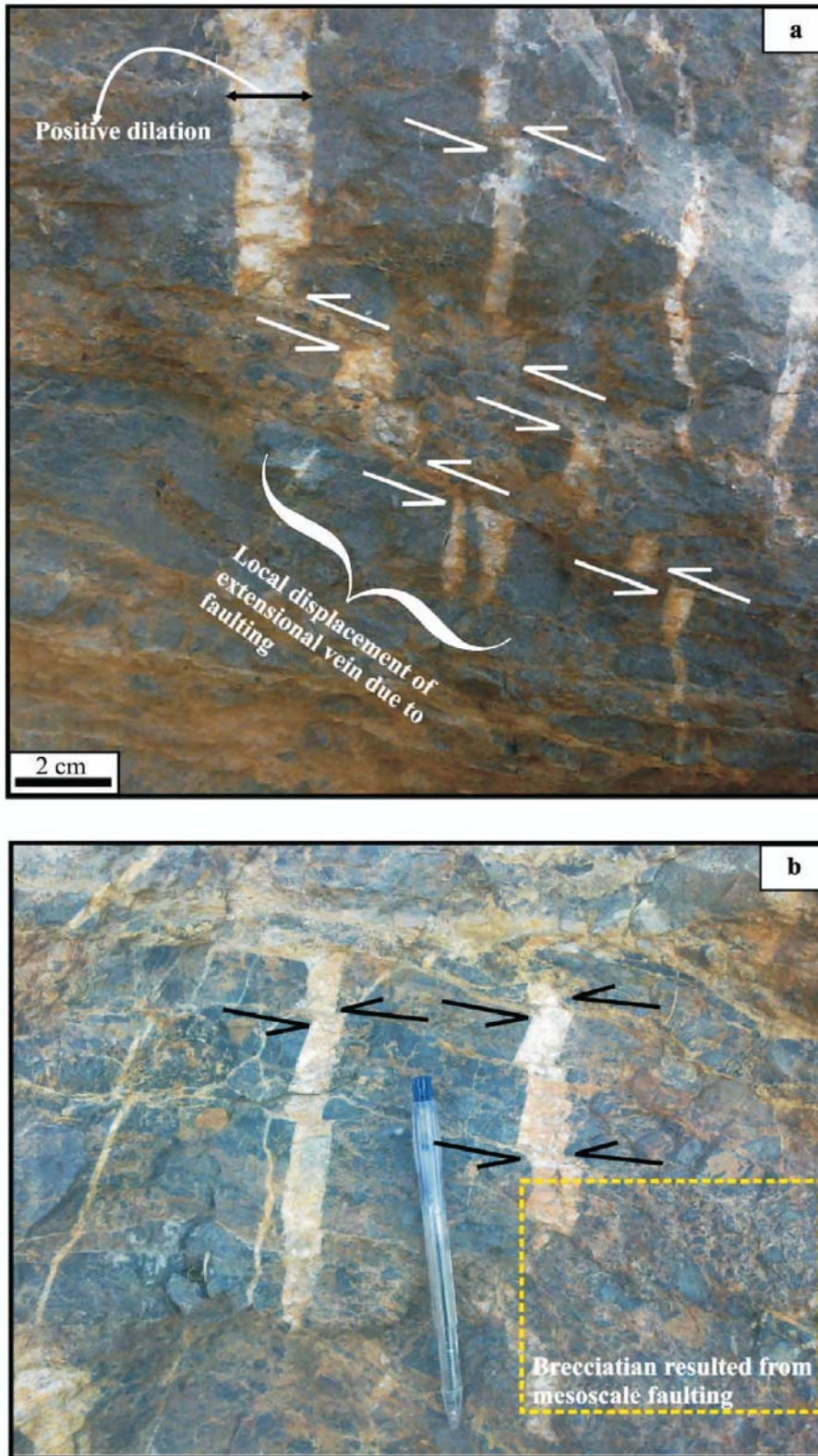
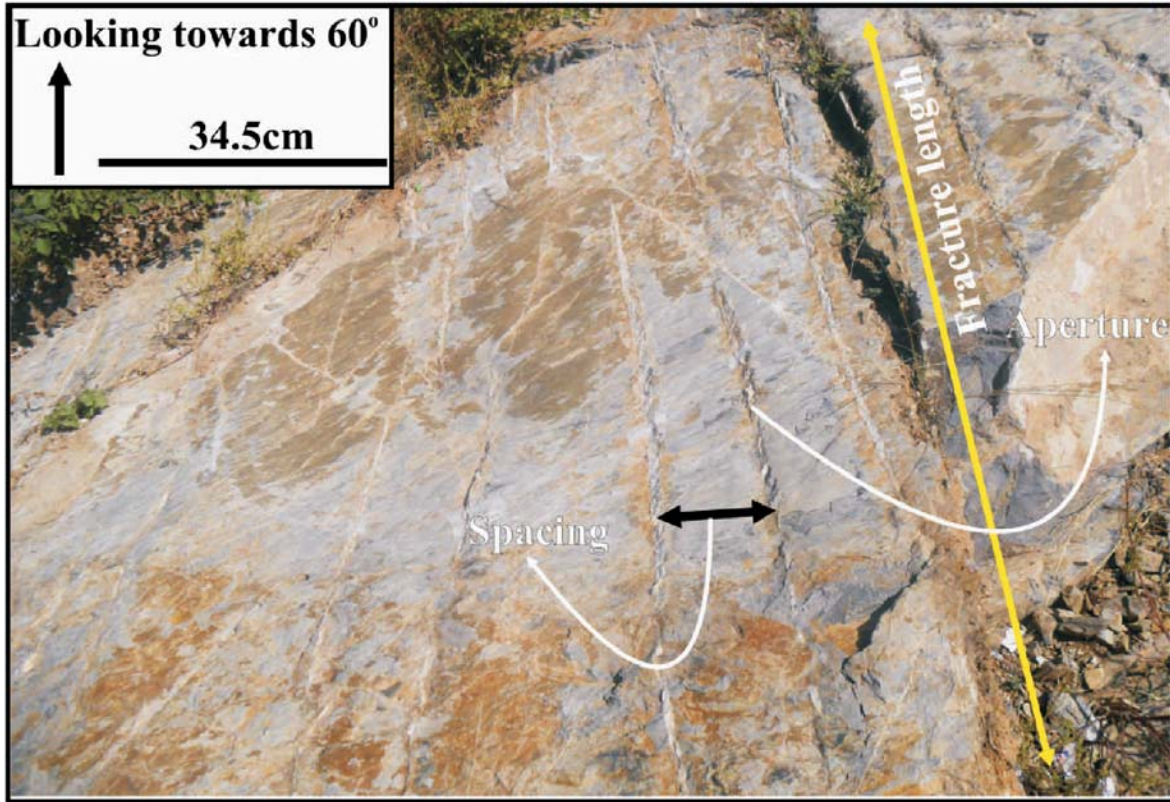


Figure 5 - Photographs (a, b) taken looking towards 50° showing deformation of tectonic veins by thrust slip faults at the inner arc of the fold shown in Figure 4.



**Figure 6 - Photograph showing through-going systematic filled fracture pattern of the Ambar Formation. The infilling materials are predominantly consists of calcite.**

Oriented samples were collected at the outcrop to study the origin of fracture microscopically by making oriented thin sections. Thin sections were made to provide sectional view normal to the fracture-faces.

#### **COLLECTIVE ILLUSTRATION OF FRACTURE DATA**

The consistent orientation patterns of the fractures of the Ambar Formation are clearly visible from the rose diagram constructed for all the fractures studied at the outcrop (Figure 8). The extension fractures trending  $\sim 50^{\circ}$ - $70^{\circ}$  make a regular and through-going fracture set.

#### **DESCRIPTION AND ANALYSES OF THE TECTONIC VEINS**

Veins of the Ambar Formation were studied mesoscopically and microscopically to evaluate their deformation history. These veins are undeformed to very slightly deformed at gently dipping beds but highly deformed at the inner arcs of the small scale folds (Figures 4a, b and 5a, b). Two types of veins were observed; continuous veins and en-echelon veins occurring in arrays (Figures 6, 9, 10 and 11). Oriented samples were systematically taken from these two types of veins. The nature and structure of their infilling materials were studied microscopically in relation to the fracture walls of the host rock.

#### **CONTINUOUS VEINS**

Dominant veins in the study area are continuous (Figure 6). They are through going, aligned in parallel sets and clearly opened in the exposed outcrops of the Ambar Formation. The estimated average mean orientation is  $\sim 50^{\circ}$ - $70^{\circ}$ . The maximum aperture of these veins is  $\sim 4.5$  cm across and with  $\sim 3$ - $10$  cm spacing between the two veins. Petrographic and textural observations collected from a vein trending  $N60^{\circ}E$  show that the vein is filled with calcite having smooth crystal boundaries (Figure 12a). Photomicrograph of the infilling material shows two crystal shapes, fibrous crystals to the right and elongate-blocky crystals to the left. The median zone is clearly marked by non-fibrous calcite crystals. The composite nature of the infilling material indicates two growth surfaces within the vein. The antitaxial growth has occurred in the fibrous part where the crystals grew to the right from the median line towards the wall rock. The syntaxial growth has occurred in elongate-blocky part of the vein where crystals grew to left from the median line. The syntaxial growth is followed by the antitaxial growth. The acute angle made by the crystal fibres with the host rock indicate oblique opening of the fracture in relation to the fracture walls but no shearing parallel to the fracture walls. The internal structure of the vein in relation to the fracture walls clearly explains the dilational movements occurred during the fracture formation. The lack of shearing effects within the vein and its relation to the

Table 2 - Fracture trends measured at 18 stations from the Ambar Formation.

Station	Dip and Azimuth	Co-ordinates	S.No	Strike
1	30° towards 315°	N 34° 02' 51.0" E 72° 24' 47.4"	1	105
			2	120
			3	65
			4	60
2	26° towards 304°	N 34° 02' 52.4" E 72° 24' 46.2"	1	175
			2	125
			3	50
			4	180
			5	110
			6	65
			7	75
			8	78
			9	15
			10	63
			11	55
3	30° towards 320°	N 34° 02' 51.3" E 72° 24' 46.9"	1	55
			2	55
			3	65
			4	60
			5	65
			6	67
			7	67
			8	65
			9	70
			10	115
			11	115
			12	115
			13	113
			4	25° towards 318°
2	105			
3	105			
4	106			
5	105			
6	65			
7	67			
8	64			
9	40			
10	20			
11	40			
5	20° towards 315°	N 34° 02' 51.4" E 72° 24' 45.5"	1	65
			2	120
			3	55
6	25° towards 340°	N 34° 02' 54.2" E 72° 24' 41.3"	1	55
			2	60
			3	58
			4	60
			5	70
			6	65
7	40° towards 290°	N 34° 03' 01.4" E 72° 24' 43.5"	1	55
			2	45
			3	45
			4	45
			5	65
			6	65
			7	50
			8	50
			9	50
			10	23
			11	23
			12	5
			13	5
			14	23
8	35° towards 280°	N 34° 02' 59.5" E 72° 24' 50.7"	1	45
			2	50
			3	100
			4	50
			5	45
			6	60
			7	65
			8	60
			9	55
			10	58
			11	95
			12	95
			13	8
			14	8
			15	10
			16	50
			17	50
			18	30
19	50			
20	60			
21	60			
9	25° towards 260°	N 34° 02' 55.9" E 72° 24' 57.9"	1	55
			2	60
			3	60
			4	55
			5	35
			6	65
			7	105
			8	100
			9	40
			10	100
			11	50
			12	60
			13	125
			14	20
			15	30
			16	60
			17	60
			18	60
			19	35
10	30° towards 330°	N34° 02'52.9" E72° 24'44.8"	1	120
			2	120
			3	100
			4	60
			5	55
			6	105
			7	10
			8	75
			9	65
			10	65
			11	50
			12	45
			13	55
			14	95
			15	20
			16	10
			17	15
			18	55
			19	15
11	35° towards 280°	N 34° 03' 06.1" E 72° 24' 45.7"	1	65
			2	65
			3	60
			4	65
12	25° towards 275°	N 34° 03' 03.2" E 72° 24' 46.2"	1	50
			2	45
			3	55
			4	95
			5	20
			6	10
13	40° towards 280°	N 34° 03' 03.4" E 72° 24' 46.8"	1	15
			2	55
			3	15
14	30° towards 250°	N 34° 02' 59.5" E 72° 24' 52.3"	1	60
			2	35
			3	100
			4	75
			5	90
15	30° towards 280°	N 34° 02' 55.6" E 72° 24' 55.2"	1	55
			2	50
			3	50
			4	110
16	35° towards 280°	N 34° 02' 54.8" E 72° 24' 56.3"	1	95
			2	95
			3	40
			4	115
17	30° towards 270°	N 34° 03' 09.3" E 72° 24' 55.5"	1	115
			2	100
			3	85
			4	95
			5	20
			6	15
			7	15
			8	165
18	30° towards 320°	N 34° 03' 03.8" E 72° 24' 36.4"	1	50
			2	50

Fracture Analyses of the Early Cambrian Ambar Formation

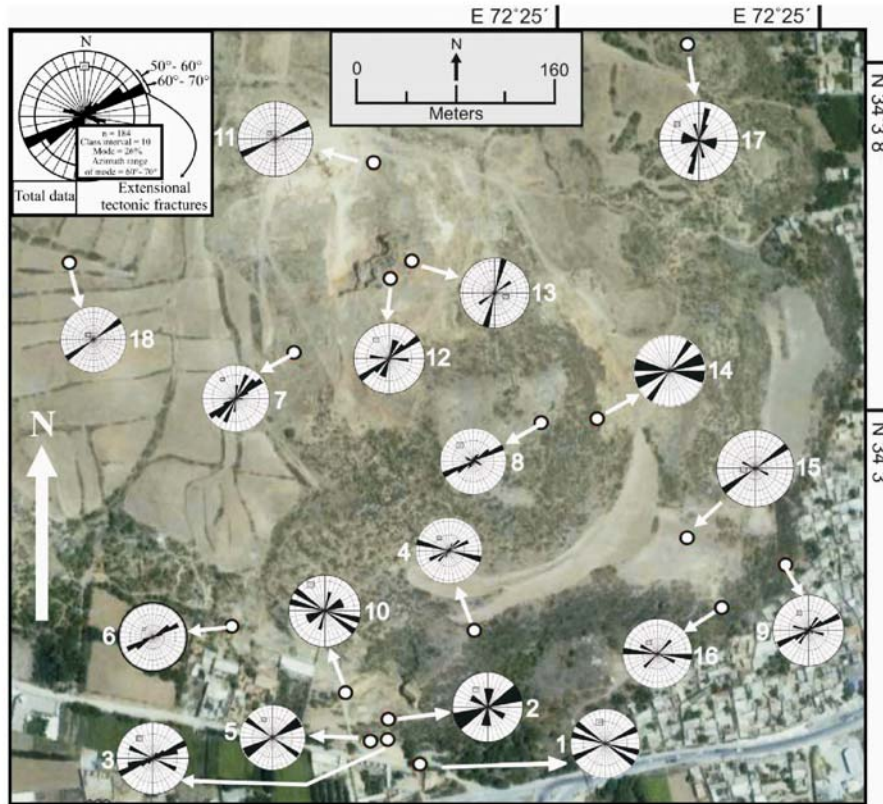


Figure 7 - Satellite image of the study area showing spatial distribution of fracture data taken at 18 stations.

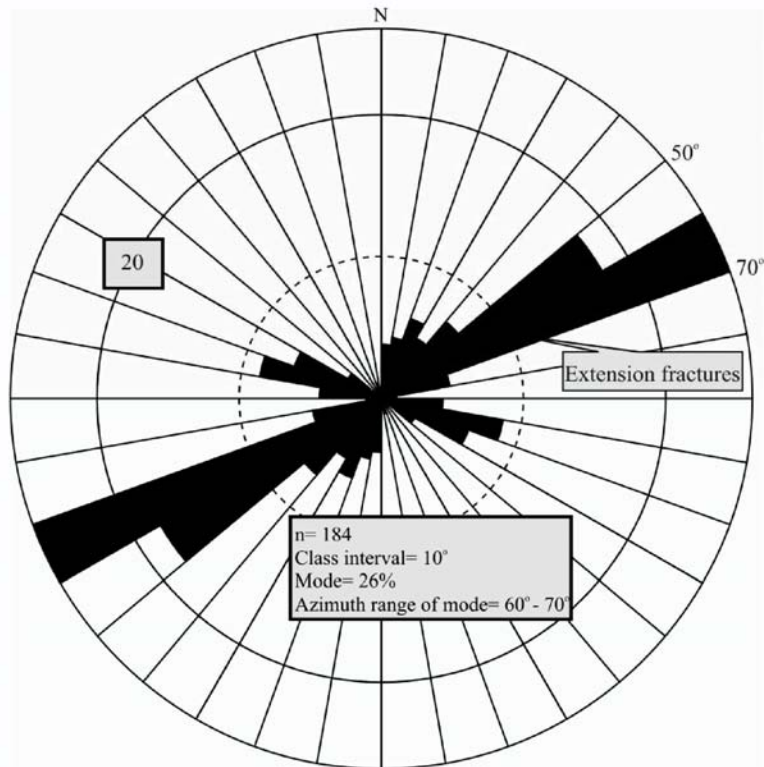


Figure 8 - Equal area rose diagram showing all fractures trends across the Ambar Formation.



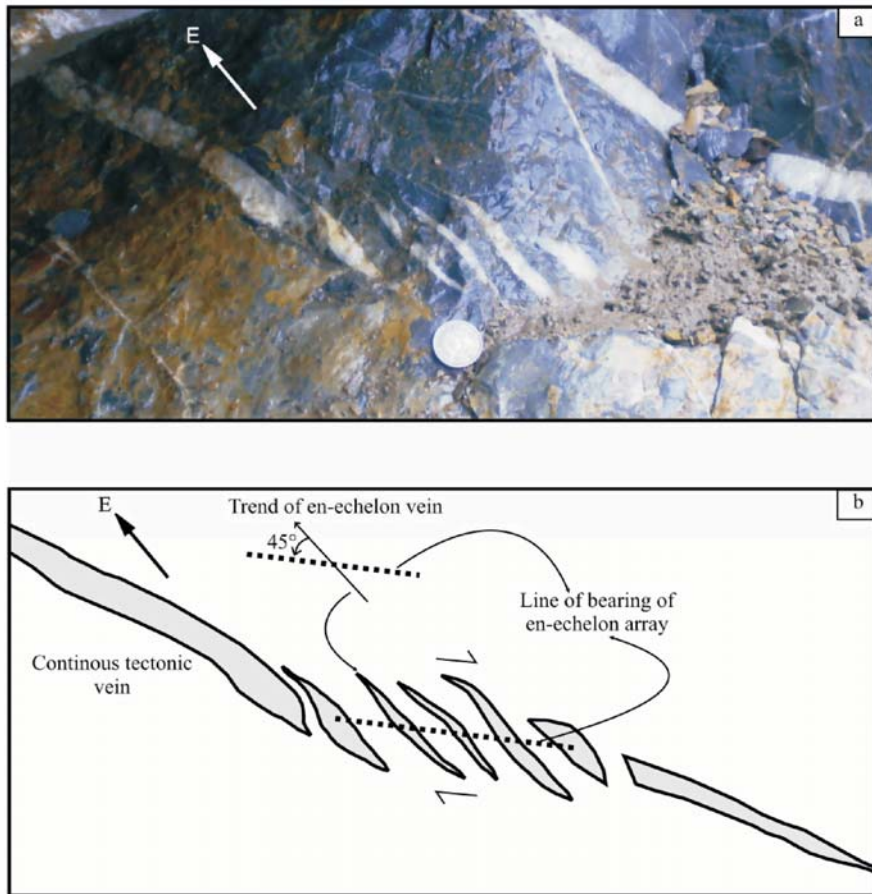


Figure 9 - Photograph (a) and line diagram (b) showing geometry of dextral en-echelon vein array and sense of shear associated with the opening and propagation of vein.

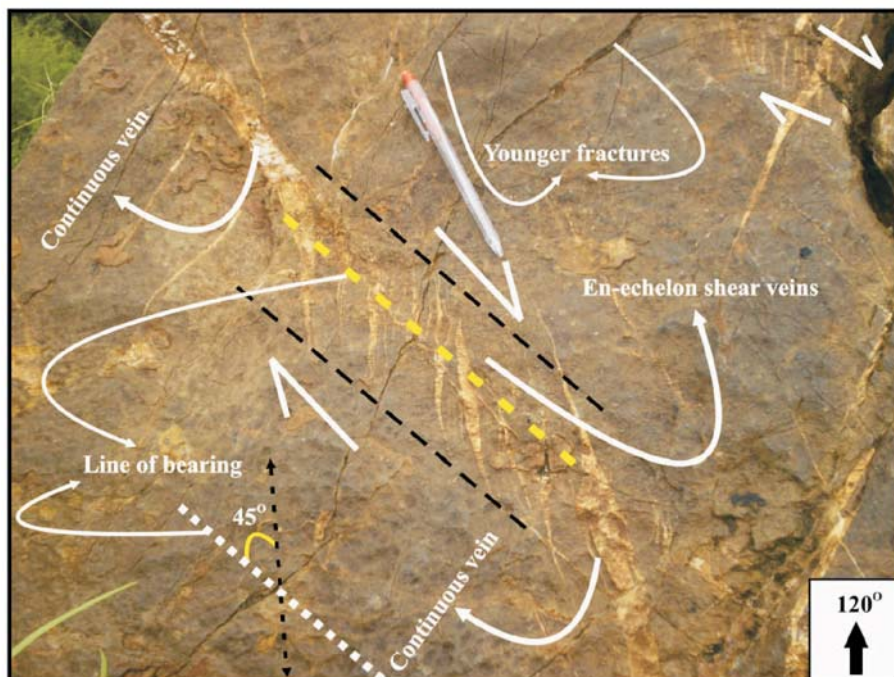


Figure 10 - Photograph showing local dextral shear zone associated with propagating continuous veins.

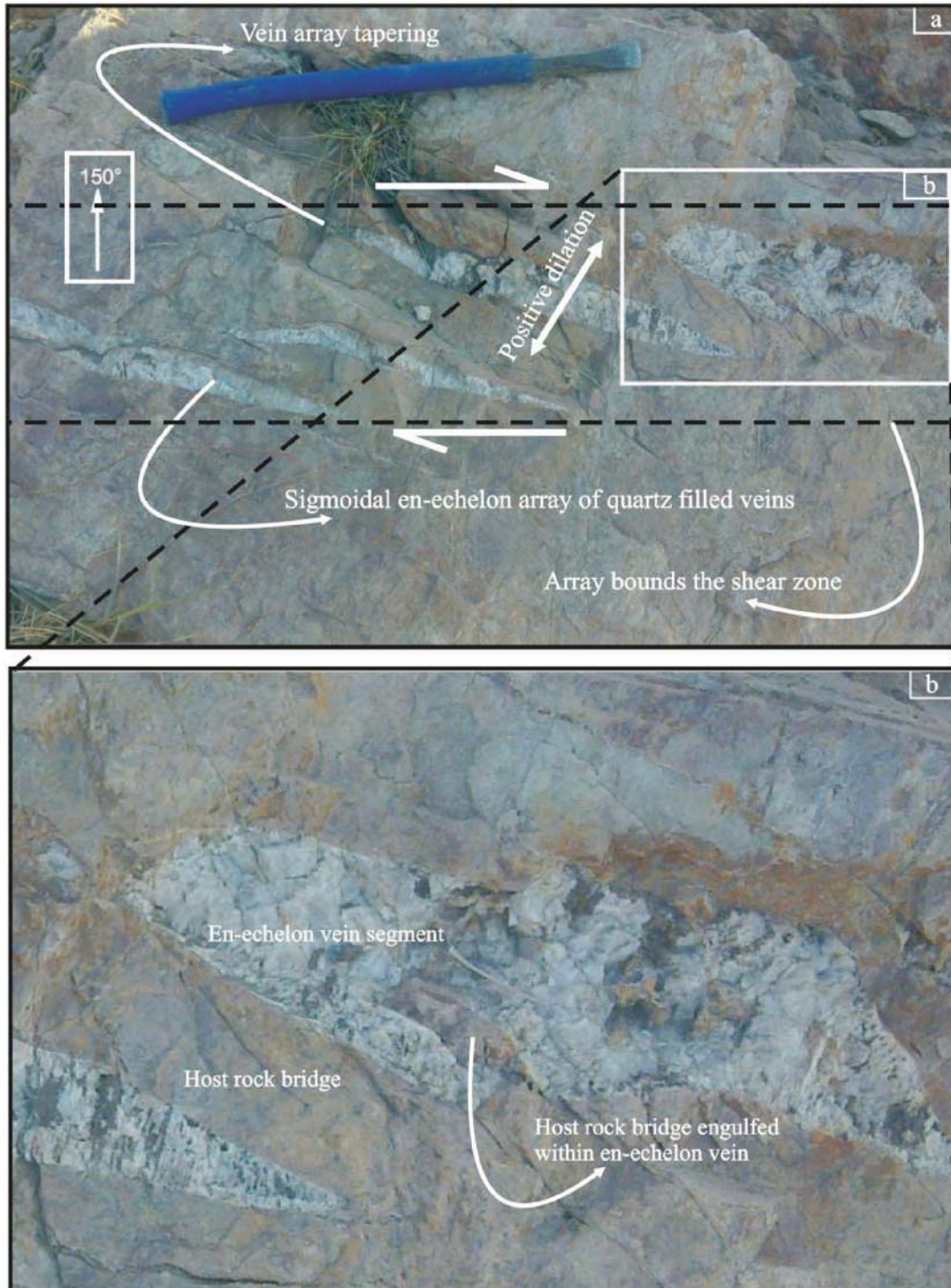


Figure 11 - (a) Photograph showing dextral en-echelon vein array; (b) Photograph demonstrating en-echelon vein, engulfing host-rock bridge in the process of linkage and propagation.

fracture walls preclude the possibility of shearing phenomenon for the formation of these veins. These extension veins are considered to have been formed in the extensional tectonic regime, accompanying the Late Paleozoic normal faulting, during intra-continental rifting.

### EN-ECHELON VEIN ARRAYS

En-echelon vein arrays form during incremental dilation at  $45^\circ$  or less to the line of bearing of the linear zone as a whole (Davis, 1984). Linkage and propagation of two formerly opened en-echelon veins result in the incorporation of host rock bridges in between them, within the newly formed vein (Figure 11; Nicholson, 1991). Sigmoidal shaped en-echelon vein arrays were observed at many places that are clearly associated with the continuous veins (Figures 9 and 10). These arrays link up with a two continuous veins on both sides. The line of bearing of the whole vein array and the trend of individual vein makes  $45^\circ$  angle with each other. The line of bearing of the array connects the two propagating continuous veins. The shear plane is parallel to the line of bearing of the array, which is making  $45^\circ$  angle with the opening vein and the shear sense is opposite to the geometric arrangement of the array (Figures 9 and 10). Host rock sigmoidal bridges and the

incorporation of host rock materials between and with in the en-echelon vein were observed respectively, which indicate shear displacement and extension of the array (cf. Nicholson, 1991; Figures 11a and 11b). Oriented sample was collected from an en-echelon vein lying between two  $N60^\circ E$  trending continuous veins. The en-echelon vein is filled with non-fibrous calcite crystals (Figure 12b), and are separated by host rock bridges, which are cut through by younger fractures (Figure 10). The geometry of the en-echelon vein array and the dilational movements inside the individual en-echelon vein both support hybrid mechanism of extension and shear fracturing for the formation of these arrays. The propagating and dilating en-echelon veins are linked together by the development of local ductile shear zones that allows opening of the en-echelon veins at  $45^\circ$  to the ductile shear plane. Thus opening of the en-echelon vein is purely a dilational activity but accompanied by the local ductile shear during the linkage and propagation.

### CONCLUSION AND INTERPRETATION

This study shows that fractures, veins and associated structures can effectively be used to decipher very complex tectonic histories of the host rocks. The compressional and

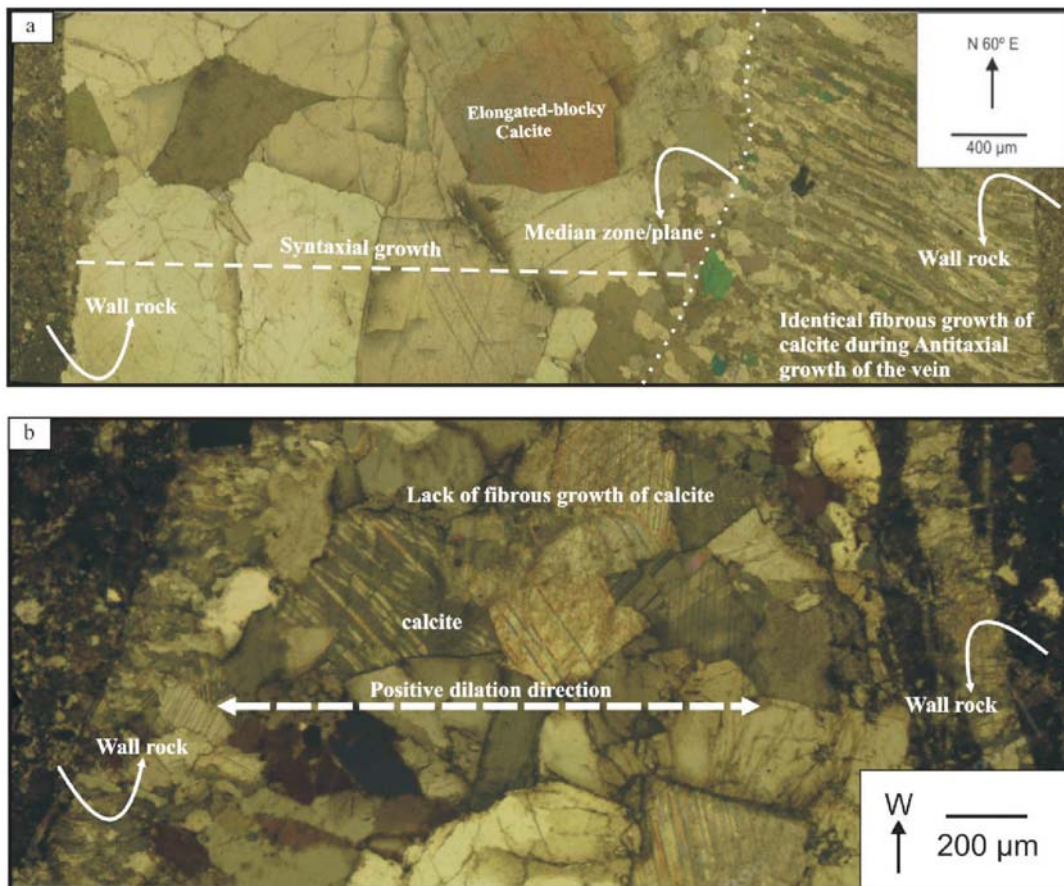


Figure 12 - . (a) Photomicrograph showing a calcite filled vein. It is a composite vein with an antitaxial fibrous part (right) where fibers grew towards the right and a syntaxial part (left) where elongate-blocky crystals grew towards the left; (b) Photomicrograph of en-echelon vein showing non-fibrous calcite infilling material.

## Fracture Analyses of the Early Cambrian Ambar Formation

extensional environments generated during tectonic activities result in distinctive fracturing of the rocks (Figure 13). The gently dipping beds of the Ambar Formation at the study area are thoroughly fractured with  $\sim 50^{\circ}$ - $70^{\circ}$  striking fracture set. These fractures are through going and sub-persistent to persistent with apertures up to 4.5 cm at places. They are filled with secondary minerals, dominantly calcite and quartz. Among all the fractures only  $\sim 50^{\circ}$ - $70^{\circ}$  trending fracture set shows regular spacing and consistent geometry and attitude.

Throughout in Ambar Formation the bed-thickness is proportional to fracture spacing. The medium bedded dolomite is regularly fractured with  $\sim 50^{\circ}$ - $70^{\circ}$  striking fracture set.  $\sim 3$ - $10$  cm of spacing is noted between the adjacent fractures. Where the subordinate thin interbeds are densely fractured and very closely spaced.

Microscopic study of the infilling secondary minerals and their internal structures in relation to fracture walls indicate that these fractures belong to Mode I extension fractures. Geometry of the en-echelon vein arrays, host rock incorporation within the en-echelon vein (associated with fracture dilation, propagation and linkage) and their crystal

growth mechanism further support the extensional nature of these fractures.

Extension fractures of the Ambar Formation reveal the early history of tectonism, which pre-dates the Cenozoic Himalayan Orogeny. However, later deformation of these fractures at the crest of outcrop scale folds occurred during the Himalayan Orogeny (Figures 4a, 4b and 5a, 5b). Note the fold axis of these micro scale folds is parallel to the Swabi Synclinorium (Figure 14). Orientation of these extensional fractures is different from the present tectonic grain of the Himalayan Orogeny across the region. The resemblance of the trends of extension fractures with the trends of the Late Paleozoic inferred normal faults and rift related intrusive bodies suggests that these fractures developed during the Late Paleozoic intra-continental rifting in Extensional tectonic regime (Figure 14).

## ACKNOWLEDGMENTS

We appreciate the fund and outstanding facilities provided by the Department of Geology, University of Peshawar for carrying on this research. We thank Muhammad Shafique for

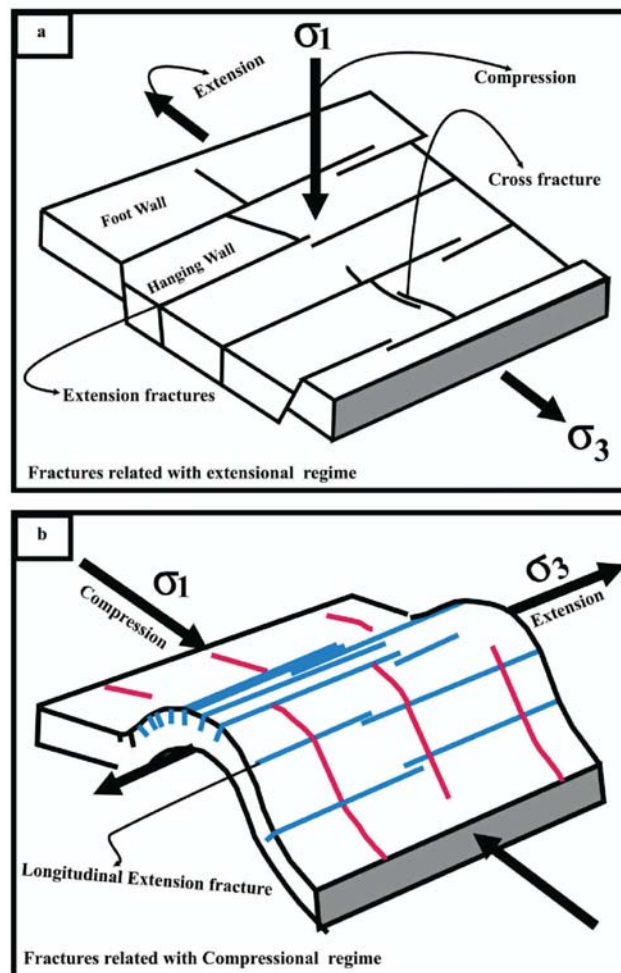


Figure 13- Schematic block diagrams showing fractures association (a) with the normal faults in an extensional tectonic setup and (b) with the folded terrains in compressional tectonic environment. Orthogonally oriented  $\sigma_1$  and  $\sigma_3$  illustrate maximum and minimum stress directions respectively (after Herman, 2005). Note the fractures become wide in the direction of  $\sigma_3$ .

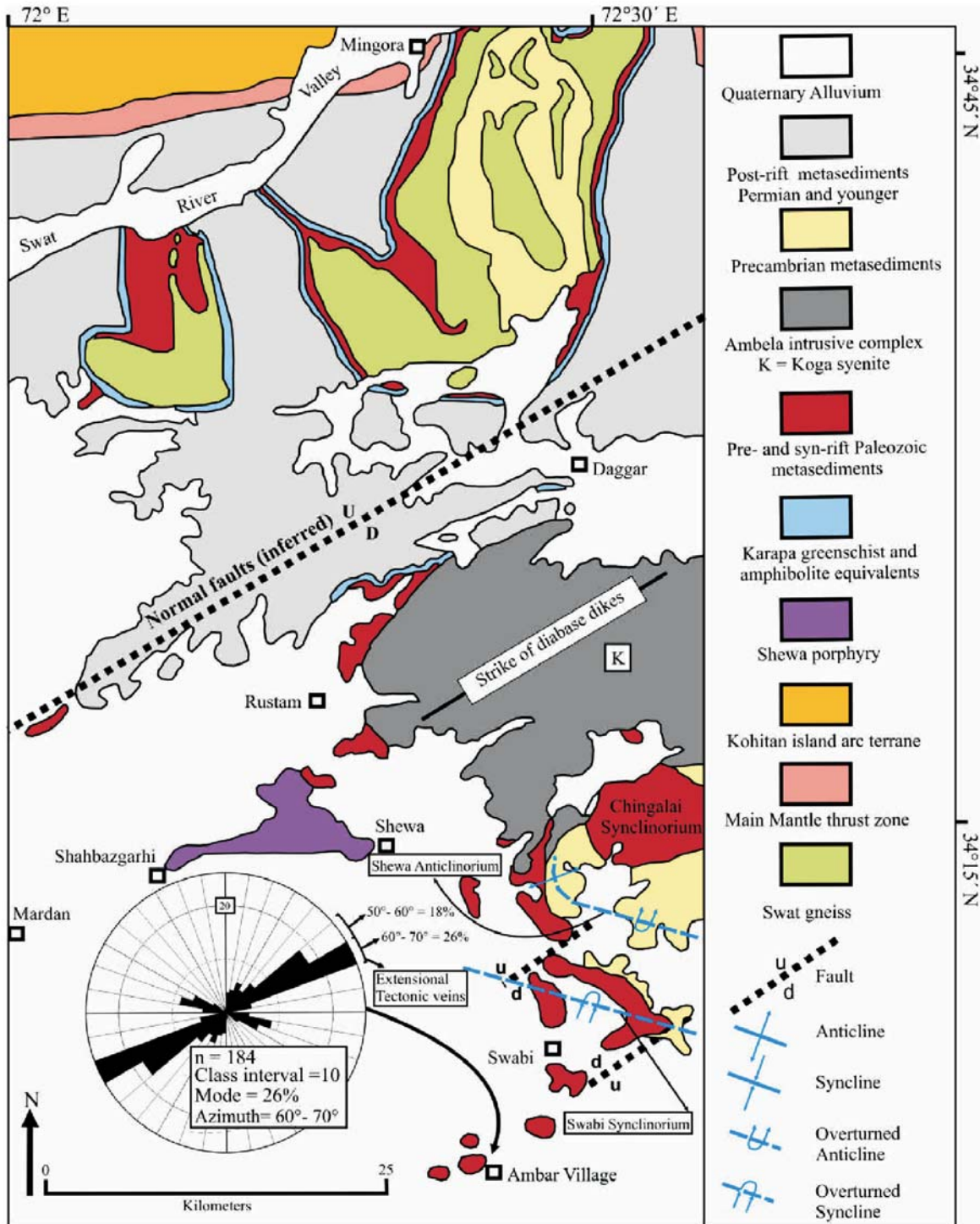


Figure 14 - Tectonic map of the eastern Peshawar Basin and south central Swat showing trends of regional scale geological structures (modified after Pogue et al., 1992a and Hussain et al., 1991). The attitudes of extension veins are shown in relation to the regional geological structures. Equal area rose diagram represents the fracture trends recorded at the study area. Trends of extension veins is almost coinciding with the trends of the normal faults and diabase dikes.

editorial management and two anonymous reviewers for their beneficial reviews of this manuscript.

## REFERENCES

- Anderson, E. M. (1951). The dynamics of faulting and dike formation. Edinburgh: Oliver and Boyd.
- Burbank, D. W. (1983). The chronology of intermontane-basin development in the north-western Himalaya and the evolution of the Northwest Syntaxis. *Earth and Planetary Science Letters*, 64, 77-92. Amsterdam: Elsevier.
- Davis, G. H. (1984). Structural geology of rocks and regions. New York: Wiley.
- Davis, G. H., and Reynolds, S. J. (1996). Structural geology of rocks and regions. New York: John Wiley and Sons.
- DiPietro, J. A., Pogue, K. R., Hussain, A., and Ahmad, I. (1999). Geologic map of the Indus syntaxis and surrounding area, northwest Himalaya, Pakistan, in Macfarlane, A., Sorkhabi, R. B. and Quade, J., (eds.), Himalaya and Tibet: Mountain roots to mountain tops: Boulder, Colorado, Geological Society of America, special paper 328.
- Engelder, T. (1982). Is there a genetic relationship between selected joints and contemporary stress within lithosphere of North America? *Tectonics*, 1, 161-177.
- Hancock, P. L. (1985). Brittle microtectonics: Principles and practice. *Journal of Structural Geology*, 7, 437-457.
- Herman, G. C. (2005). Joints and veins in the Newark basin, New Jersey, in regional tectonic perspective: I Gates, A. E., editor, Newark Basin View from the 21st Century, 22nd Annual Meeting of the Geological Association of New Jersey, College of New Jersey, Ewing, New Jersey, 75-116.
- Hussain, A., Pogue, K. R., Khan, S. R., and Ahmad, I. (1991). Paleozoic stratigraphy of the Peshawar basin. *Geological Bulletin*, University of Peshawar, 24, 85-97.
- Jaeger, J. C., and Cook, N. G. W. (1979). *Fundamentals of Rock Mechanics*. London: Chapman and Hall.
- Kazmi, A. H., and Jan, M. Q. (1997). *Geology and Tectonics of Pakistan*. Karachi, Pakistan: Graphic.
- Koehn, D., Arnold, J., and Passchier, C. W. (2005). Fracture and vein patterns as indicators of deformation history: a numerical study: Geological Society, London, Special Publications, 243, 11-24.
- Nicholson, R. (1991). Vein morphology, host rock deformation and the origin of the fabrics of en-echelon mineral veins. *Journal of Structural Geology*, 13(6), 635-641.
- Oliver, N. H. S., and Bons, P. D. (2001). Mechanisms of fluid flow and fluid-rock interaction in fossil metamorphic hydrothermal systems inferred from vein wall rock patterns, geometry and microstructure. *Geofluids*, 1, 137-163.
- Ori, G. G., and Friend, P. F. (1984). Sedimentary basins formed and carried piggyback on active thrust sheets. *Geology*, 12, 475-478.
- Parker, J. M. (1942). Regional systematic jointing in slightly deformed sedimentary rocks. *Geological Society of America, Bulletin*, 53, 381-408.
- Paterson, M. S. (1978). *Experimental Rock Deformation - Brittle Field*. Berlin: Springer-Verlag.
- Pivnik, D. A., and Wells, N. A. (1996). The transition from Tethys to the Himalaya as recorded in northwest Pakistan. *Geological Society of America, Bulletin*, 108, 1295-1313.
- Pogue, K. R., DiPietro, J. A., Khan, S. R., Hughes, S. S., Dilles, J. H., and Lawrence, R. D. (1992a). Late Paleozoic rifting in northern Pakistan. *Tectonophysics*, 11, 871-883.
- Pogue, K. R., Hylland, M. D., Yeats, R. S., Khattak, W. U., and Hussain, A. (1999). Stratigraphic and structural framework of Himalayan foothills, Northern Pakistan. In: Macfarlane, A., Sorkhabi, R. B. and Quade, J., (eds.), Himalaya and Tibet: Mountain roots to Mountain tops: Boulder, Colorado. Geological Society of America, Special paper 328.
- Pogue, K. R., Wardlaw, B. R., Harris, A. G., and Hussain, A. (1992b). Paleozoic and Mesozoic stratigraphy of the Peshawar basin, Pakistan: Correlations and implications. *Geological Society of America, Bulletin*, 104, 915-927.
- Pollard, D. P., and Aydin, A. (1988). Progress in understanding jointing over the past century. *Geological Society of America, Bulletin*, 100, 1181-1024.
- Price, N. J., and Cosgrove, J. W. (1990). *Analysis of Geological Structures*. Cambridge: Cambridge University Press.
- Ramsay, J. G. (1967). *Folding and fracturing of rocks*. New York: McGraw Hill Books.
- Ramsay, J. G. (1980). Shear zone geometry: A review. *Journal of Structural Geology*, 2, 83-99.
- Ramsay, J. G., and Huber, M. I. (1987). *The techniques of modern structural geology, 2: Folds and fractures*. London, England: Academic Press.
- Ramsey, J. M., and Chester, F. M. (2004). Hybrid fracture and the transition from extension fracture to shear fracture. *Nature*, 428, 63-66.
- Ranalli, G. (1995). *Rheology of the Earth (2nd edn)*. London, England: Chapman and Hall.
- Treloar, P. J., Broughton, R. D., Williams, M. P., and Khan, M. A. (1989). Deformation, metamorphism and imbrication of the Indian plate south of the Main Mantle thrust, North Pakistan. *Journal of Metamorphic Geology*, 7, 111-125.
- Twiss, R. J., and Moores, M. (1992). *Structural Geology*. New York: Freeman and Company.
- Yeats, R. S., and Lawrence, R. D. (1984). Tectonics of the Himalayan thrust belt in Northern Pakistan. In: Haq, B. U., and Milliman, J. D., (eds.), *Marine geology and oceanography of Arabian sea and coastal Pakistan*. New York: Van Nostrand Reinhold, 177-198.

PJHR

Received Dec. 21, 2011 revised March 12, 2012 and accepted May 25, 2012.